Imaging Condition for Converted Waves Based on Decoupled Elastic Wave Modes

Chenlong Wang, Jiubing Cheng, Tongji University, and Børge Arntsen, NTNU

SUMMARY

Elastic reverse time migration is developed for better characterization of the subsurface using multi-component data. Typically, imaging condition is applied to the pure P- and S-wave fields separated by the divergence and curl operators in isotropic media. However, the separated P- and S-wave fields are scalar and vector wavefields, respectively. Directly cross-correlating the P-wave mode with components of S-wave cannot obtain unique scalar image. A scalarization step is needed to implement converted wave imaging. Meanwhile, the polarity reversal in converted wave imaging causes destructive interference during stacking. We propose a new imaging condition for converted waves based on the decoupled vector wavefields. It automatically solves the polarity reversal issue. Synthetic 2D and 3D examples demonstrate the validity of this approach.

INTRODUCTION

Driven by the increasing capacity of computation, elastic reverse time migration (ERTM) is becoming feasible to the industry. It provides more opportunities for structure imaging and elastic parameter estimation compared to the acoustic migration for both isotropic and anisotropic media (Stewart et al., 2002).

Compared to separating multi-component data into single mode and then processed by extensions of techniques used for scalar and acoustic wave fields (Dankbaar, 1985; van der Baan, 2006; Sun et al., 2006), using whole vector data for ERTM has shown some promises (Yan and Sava, 2008; Zhang and McMechan, 2011; Ravasi and Curtis, 2013; Du et al., 2014; Duan and Sava, 2014; Wang et al., 2014). Yan and Sava (2008) suggested to apply cross-correlation imaging condition on pure P and S wave modes separated by the divergence and curl operators. Using the direction information during the source side wavefields reconstruction, Zhang and McMechan (2011) proposed a workflow for ERTM in angle domain. With the help of efficient wave mode separation algorithm in anisotropic media, Wang et al. (2014) extended Zhang and McMechan (2011)'s method by applying cross-correlation imaging condition.

There are two issues when working on the ERTM: First, the separated pure P- and S-wave by the divergence and curl operators are scalar and vector wavefields, respectively. Therefore, a scalarization method is needed to handle the S wavefields for applying cross-correlation imaging condition. Without it, the PS or SP migration result will have three components at every image point (Yan and Sava, 2008); Second, the polarity of S wave will flip at the normal incident point which makes destructive contribution to the stacked migrated result.

In 2D case (in xz plane), the separated vector S-wave fields only has one component in the y direction. It is always taken as scalar wavefields to avoid vector imaging. Meanwhile, this unique component contains the polarity information of the S-wave fields. As consequence, the single shot PS migration result contains the polarity reversals. Methods to correct the polarity reversal depend on the incident angle with respect to the normal of the interface. It can be implemented either in the imaging space domain (Du et al., 2012; Duan and Sava, 2014) or in the angle gathers (Rosales and Rickett, 2001). In 3D case, this issue comes to be more complex. Du et al. (2014) gave a method to define a reference direction based on the Poynting vector and then project the separated vector S wavefields on it to validate the scalar imaging. Instead of using the direction information from the receiver sides, Duan and Sava (2014) proposed an imaging condition exploits the incident direction information and the normal of the interface.

In this paper, we propose an new imaging condition for converted wave using the decoupled vector P- and S-wave fields, which contain polarity information of each mode. This approach avoids the migration artifacts from cross-talk of different wave modes and is immune to the polarity reversal for converted wave migration. It can be applied in both isotropic and anisotropic media.

IMAGING CONDITION BASED ON THE DIVERGENCE AND CURL OPERATORS

Accurate wave mode separation prior to applying imaging condition is needed to avoid the cross-talk artifacts in ERTM. In isotropic media, the separation of the elastic displacement wavefields $\mathbf{u}$ by the divergence and curl operator is given as (Aki and Richards, 2002):

$$P(\mathbf{x},t) = \nabla \cdot \mathbf{u}(\mathbf{x},t), \tag{1}$$

$$\mathbf{S}(\mathbf{x},t) = \nabla \times \mathbf{u}(\mathbf{x},t). \tag{2}$$

where, $\mathbf{x} = \{x,y,z\}$ represents the spatial coordinate. The separated P and $\mathbf{S}$ are scalar and vector wavefields, respectively. They are related with the propagation of potential wavefields as follows (Ikelle and Amundsen, 2005):

$$\begin{aligned} \partial_t^2 \chi(\mathbf{x},t) &= v_p^2 P(\mathbf{x},t), \\ \partial_t^2 \mathbf{\Phi}(\mathbf{x},t) &= -v_s^2 \mathbf{S}(\mathbf{x},t). \end{aligned} \tag{3}$$

where, χ and $\mathbf{\Phi}$ are *Lamé* potentials which connect with the displacement wavefields by the Helmholtz decomposition:

$$\mathbf{u} = \nabla\chi + \nabla \times \mathbf{\Phi} = \mathbf{u}_p + \mathbf{u}_s, \tag{4}$$

in which, $\mathbf{u}_p$ and $\mathbf{u}_s$ are the particle displacements of P- and S-wave, respectively. Figure 1 is shown to illustrate the local wave propagation in 3D case. We consider a reflector denoted as I at the bottom side of the illustration cube. A P wave source emits energy outward from the top side of the cube. Vectors $\mathbf{D}_p$ and $\mathbf{D}_s$ are the raypath of incident P-wave and reflect S-wave, respectively. They are belong to the reflection plane Ψ

DOI http://dx.doi.org/10.1190/segam2015-5920952.1

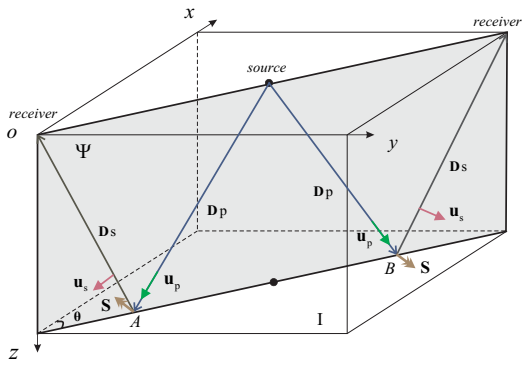

Figure 1: Cartoon describing converted PS-wave propagation in 3D elastic media.

which has an angle θ with respect to the x-axis in a clockwise direction. The reflection points A and B are on the different sides of *source*. The green and red arrows denote the P- and S-wave displacement vectors, respectively. For isotropic media, they are within the reflection plane as well. The brown arrow represents the separated vector $\mathbf{S}$ with the curl operator. It is perpendicular to both the vector $\mathbf{D}_s$ and displacement vector $\mathbf{u}_s$. Therefore, it is orthogonal to the reflection plane Ψ as well.

From the physical point of view, the scalar wavefields, P, stands for the displacement flux in an unit area. It also represents the volumetric strain in the elastodynamics. As a scalar fields, it isn't responsible for the flip of polarity in migration result. Whereas, the separated vector wavefields, $\mathbf{S}$, stands for the double of *angular displacement* vector (similar with the angular velocity) due to the infinitesimal relative rotation of particles. Its magnitude indicates the size of tangential displacement (i.e. S wave) and its sign represents the tangential displacement direction (i.e. clockwise or anti-clockwise) which satisfies the right hand rule (Miklowitz, 2012). Typically, imaging condition is applied on the wavefields P and $\mathbf{S}$ separated by equation 1 and 2 (Yan and Sava, 2008; Duan and Sava, 2014; Du et al., 2014). For 2D case, the S-wave only has one component in the y direction. So regarding the converted wave imaging, Yan and Sava (2008) suggested to use the imaging condition as follows:

$$I_{ps}(\mathbf{x}) = \sum_{s}^{nshot} \int_0^{tmax} P^{src}(\mathbf{x},t;s)\, S_y^{rec}(\mathbf{x},t;s)\, dt, \qquad (5)$$

where, s is the index of shots, the superscript *src* and *rec* indicate the reconstructed wavefields from the source and receiver sides, respectively. On different sides of normal incident point, due to the symmetry of local wave propagation, the tangential displacement (S-wave) is in opposite directions. Therefore, correlation with S_y has polarity change on different sides of normal incident point. An additional polarity correction is needed before stacking. In 3D case, the vector $\mathbf{S}$ is not fixed in the y direction, it can point into any direction, which depends on the local reflection plane. In conventional implementation, a scalarization is needed before imaging. Furthermore, the reflection coefficients is defined either on potential or displacement wavefields. Thus a further correction is needed because the P and $\mathbf{S}$ wavefields have their own physical meanings as discussed above.

IMAGING CONDITION BASED ON THE VECTOR DECOMPOSITION

Instead of using the scalar P and vector $\mathbf{S}$-wave fields, we propose a new imaging condition based on decoupled vector displacement wavefields for solving the polarity reversal. The polarity reversal is depend on the geometry of local reflection relation. In isotropic media, the vector $\mathbf{S}$ wave is perpendicular to the reflection plane. Therefore, it is impossible to correct the polarity just depend on the P and the $\mathbf{S}$ wavefields. As comparison, we give following imaging conditions based on the separated displacement wavefields $\mathbf{u}_p$ and $\mathbf{u}_s$ for converted wave migration in 3D case:

$$I_{ps}(\mathbf{x}) = \int_0^{tmax} \mathbf{u}_p^{src}(\mathbf{x},t) \cdot \mathbf{u}_s^{rec}(\mathbf{x},t)dt/\Theta, \qquad (6)$$

$$\Theta = \int_0^{tmax} \mathbf{u}_p^{src}(\mathbf{x},t) \cdot \mathbf{u}_p^{src}(\mathbf{x},t)dt, \qquad (7)$$

where, Θ represents the illumination of P-wave from source side. In isotropic media, the vector $\mathbf{u}_p$ and $\mathbf{u}_s$ are both within the reflection plane Ψ.

Regarding the TI media, the geometry of converted reflection becomes more complex. In general, the raypath of incident qP wave, $\mathbf{D}_p$, is not parallel with the polarization direction. However, the polarity flips at the normal incident point with respect to the polarization direction, which is automatically given by the vector fields of qP and qSV waves. Therefore, Both in isotropic and anisotropic media, the separated vector wavefields implicitly contain the polarity information in the vicinity of incident point. Fortunately, the polarization direction of incident P-wave and reflect S-wave are changed consistently on different sides of normal incident point. As consequence, the proposed imaging condition (i.e. the dot product of decoupled wavefields) owns uniform sign in single shot imaging result.

The vector decomposition from the displacement fields can be realized as follows:

Isotropy: For separating pure mode vector wavefields with true amplitude, we can implement it in the Fourier domain (Zhang and McMechan, 2010):

$$\mathbf{u}_p(\mathbf{x}) = \int e^{i\mathbf{k}\mathbf{x}} \bar{\mathbf{k}} \left(\bar{\mathbf{k}} \cdot \widetilde{\mathbf{u}}(\mathbf{k})\right) d\mathbf{k}, \qquad (8)$$

$$\mathbf{u}_s(\mathbf{x}) = -\int e^{i\mathbf{k}\mathbf{x}} \bar{\mathbf{k}} \times \bar{\mathbf{k}} \times \widetilde{\mathbf{u}}(\mathbf{k}) d\mathbf{k}, \qquad (9)$$

where $\mathbf{k} = \{k_x, k_y, k_z\}$ is the wave-number vector and $\bar{\mathbf{k}}$ is the normalized wave-number vector. $\widetilde{\mathbf{u}}(\mathbf{k})$ is the displacement wavefields transformed into the wave-number domain. The forward and inverse Fourier transform is needed in every imaging time step. An alternative to realize it in space domain as follows:

$$\mathbf{u}_p(\mathbf{x}) \approx -\nabla\left(\nabla \cdot \mathbf{u}(\mathbf{x})\right), \qquad (10)$$

$$\mathbf{u}_s(\mathbf{x}) \approx -\nabla \times \nabla \times \mathbf{u}(\mathbf{x}). \qquad (11)$$

DOI http://dx.doi.org/10.1190/segam2015-5920952.1

Thus we can easily calculate the approximate separated vector wavefields which don't preserve the amplitude of displacement fields. As discussed by Sun et al. (2004), the separated wavefields by the divergence operator has $\pi/2$ phase shift. Therefore, there is an additional negative sign in equation 10.

Anisotropy: In homogeneous transverse isotropic (TI) media, vector displacement wavefields can be decoupled in the Fourier domain similar with the equations 8 and 9 with substituting the wavenumber vector, $\mathbf{k}$, by polarization vector of the given wave modes. The polarization vector, however, is material-dependent. It needs to be determined by solving the *Christoffel* equation. Furthermore, for heterogeneous TI media, the vector decomposition operators are in form of the mixed-domain Fourier integral operators. They can be given as follows (Cheng and Fomel, 2014):

$$\mathbf{u}_m(\mathbf{x}) = \int e^{i\mathbf{k}\mathbf{x}} \mathbf{a}_m(\mathbf{x},\mathbf{k}) \left[\mathbf{a}_m(\mathbf{x},\mathbf{k}) \cdot \tilde{\mathbf{u}}(\mathbf{k})\right] d\mathbf{k}. \qquad (12)$$

Where $\mathbf{a}_m$ represents the normalized polarization vector of wave mode $m = [qP, qSV]$. Direct solving these equations are extremely expensive. With low-rank decomposition of the integral operators, we can achieve mode decoupling efficiently for heterogeneous TI media (Cheng and Fomel, 2014).

EXAMPLES

We first test our new imaging condition on a 2D two-layer VTI model (Figure 2(a)), in which the first layer with $v_{p0} = 2400m/s$, $v_{s0} = 1380m/s$, $\varepsilon = 0.14$ and $\delta = 0.08$, and the second layer $v_{p0} = 3200m/s$, $v_{s0} = 1800m/s$, $\varepsilon = 0.2$ and $\delta = 0.1$. An anisotropic P-wave source (Wang et al., 2015) is put in the middle of the surface. Figure 2(b) and 2(c) illustrate the x- and z-components of vector qP-wave from the source side, respectively. Figure 2(d) and 2(e) show the x- and z-components of vector qSV-wave from the receiver side. Figure 2(f) shows single shot PS imaging result by the conventional imaging condition. It is obtained by cross-correlating the pure wavefields separated by divergence-like and curl-like operators in anisotropic media. Compared with the conventional imaging result, the PS imaging by our new imaging condition (Figure 2(g)) is immune to the polarity reversal.

We also test our method on a 3D isotropic two-layers model (Figure 3(a)). A horizontal reflector is located at the depth of 150m. Similar with previous example, Figure 3(b), 3(c), 3(d) and Figure 3(e), 3(f), 3(g) demonstrate the three components of P wave from the source side and S wave from the receiver side, respectively. Figure 3(h) is the PS imaging result with our new imaging condition. It doesn't need a scalarization step for S wave anymore and the result is immune to the polarity reversal as well.

The last example is tested on part of the modified 2D SEG/EAGE overtrust model(Figure 4(a)). We simulated 80 shots on the top of this model and with largest offset of 2km. For converted wave images, as shown in Figure 4(b) the migrated interfaces is destructed during stacking due to the polarity reversal. As comparison, the PS migration result by our imaging condition (Figure 4(c)) is more clear and continuous. Some artifacts in both imaging results are caused by the acquisition aperture effects.

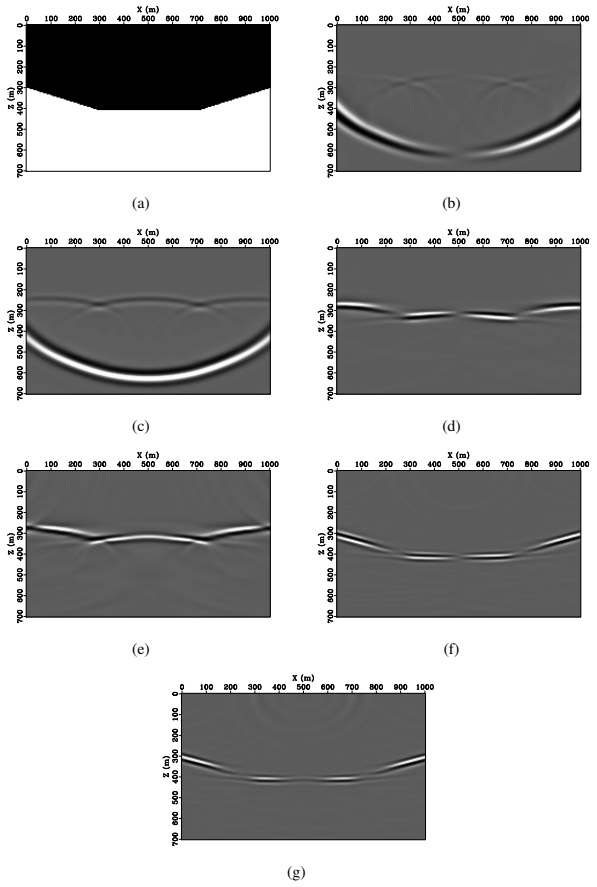

Figure 2: A 2D synthetic example: (a) a VTI model with one horizontal reflector; (b)x- and (b) z-component of $\mathbf{u}_p$ from source side; (c) x- and (d) z-component of $\mathbf{u}_s$ from receiver side; Single shot PS imaging with conventional imaging condition (e) and the new imaging condition (f).

CONCLUSION

We propose an imaging condition for converted waves imaging in 2D and 3D ERTM, in which the decoupled vector P- and S-wave fields are cross-correlated. In the vicinity of reflection point, the polarization directions of incident P- and reflected S-wave modes are changed simultaneously. Therefore, Our imaging condition avoids the cross-talk artifacts and is immune to the polarity reversal automatically. Numerical examples in 2D and 3D cases illustrate the feasibility of this method.

ACKNOWLEDGEMENT

This work was supported by the China Scholarship Council (No.201406260132), the National Natural Science Foundation

DOI http://dx.doi.org/10.1190/segam2015-5920952.1

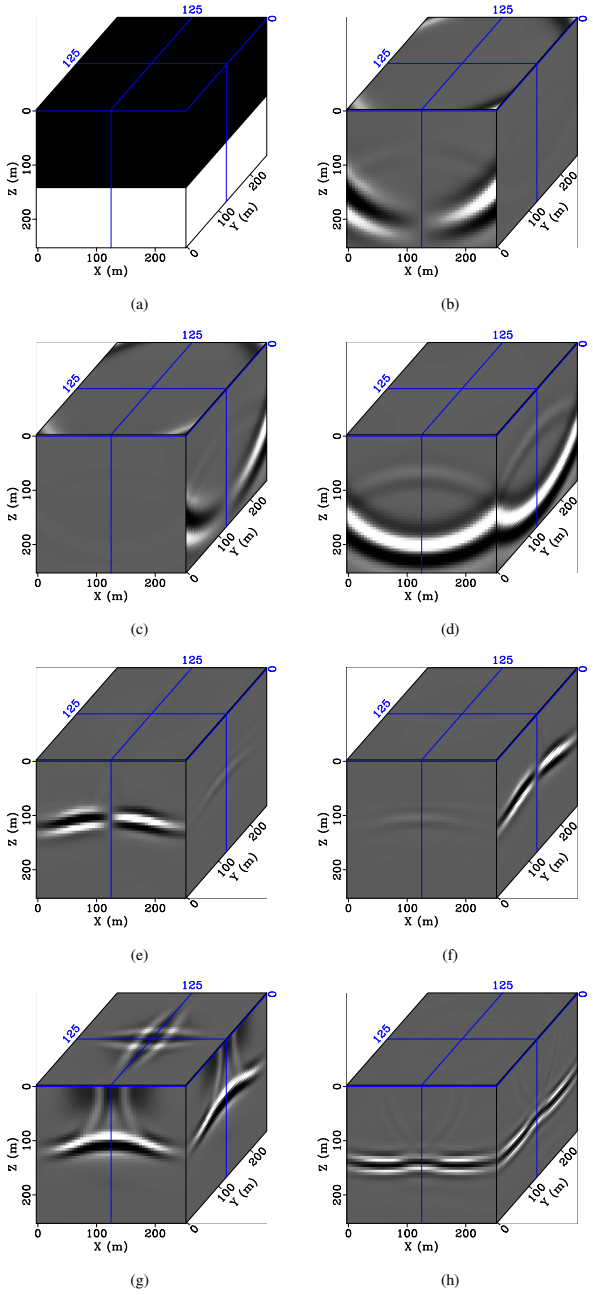

Figure 3: A 3D synthetic example: (a) an isotropic model with one horizontal reflector; (b) x- , (c) y- and (d) z-component of $\mathbf{u}_p$ from source side; (e) x- , (f) y- and (g) z-component of $\mathbf{u}_s$ from receiver side; (h) Single shot PS imaging result with new imaging condition;

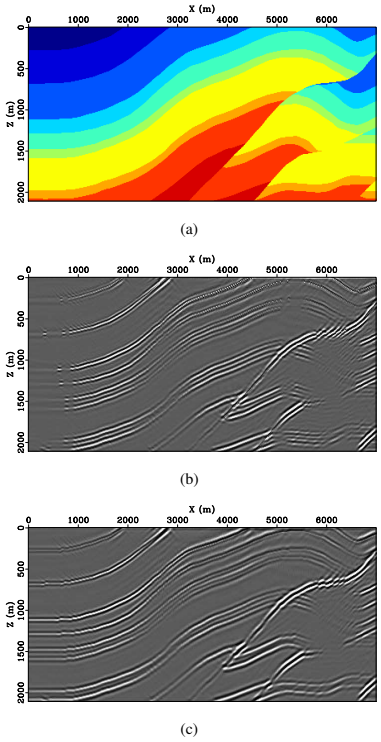

Figure 4: A 2D complex model: (a) part of SEG/EAGE overtrust model; PS imaging results by (b) conventional imaging condition and (c) our new imaging condition.

of China (No.41474099) and Shanghai Natural Science Foundation (No.14ZR1442900). C.L. Wang would like to thank W. Weibull and T.F. Wang for interesting and helpful discussions. We appreciate the ROSE consortium for providing the computation and working environment and acknowledge the support of the Madagascar open-source package (Fomel et al., 2013).

DOI http://dx.doi.org/10.1190/segam2015-5920952.1

EDITED REFERENCES

Note: This reference list is a copyedited version of the reference list submitted by the author. Reference lists for the 2015 SEG Technical Program Expanded Abstracts have been copyedited so that references provided with the online metadata for each paper will achieve a high degree of linking to cited sources that appear on the Web.

REFERENCES

Aki, K., and P. G. Richards, 2002, Quantitative seismology: Theory and methods: University Science Books.

Cheng, J., and S. Fomel, 2014, Fast algorithms for elastic-wave-mode separation and vector decomposition using low-rank approximation for anisotropic media: Geophysics, **79**, no. 4, C97–C110. http://dx.doi.org/10.1190/geo2014-0032.1.

Dankbaar, J., 1985, Separation of P- and S-waves: Geophysical Prospecting, **33**, no. 7, 970–986. http://dx.doi.org/10.1111/j.1365-2478.1985.tb00792.x.

Du, Q., X. Gong, M. Zhang, Y. Zhu, and G. Fang, 2014, 3D PS-wave imaging with elastic reverse-time migration: Geophysics, **79**, no. 5, S173–S184. http://dx.doi.org/10.1190/geo2013-0253.1.

Du, Q., Y. Zhu, and J. Ba, 2012, Polarity reversal correction for elastic reverse-time migration: Geophysics, **77**, no. 2, S31–S41. http://dx.doi.org/10.1190/geo2011-0348.1.

Duan, Y., and P. Sava, 2014, Converted-waves imaging condition for elastic reverse-time migration: 84th Annual International Meeting, SEG, Expanded Abstracts, http://dx.doi.org/10.1190/segam2014-1289.1.

Fomel, S., P. Sava, I. Vlad, Y. Liu, and V. Bashkardin, 2013, Madagascar: Open-source software project for multidimensional data analysis and reproducible computational experiments: Journal of Open Research Software, **1**, no. 1, e8. http://dx.doi.org/10.5334/jors.ag.

Ikelle, L. T., and L. Amundsen, 2005, Introduction to petroleum seismology: SEG. http://dx.doi.org/10.1190/1.9781560801702.

Miklowitz, J., 2012, The theory of elastic waves and waveguides: Elsevier.

Ravasi, M., and A. Curtis, 2013, Nonlinear scattering based imaging in elastic media: Theory, theorems, and imaging conditions: Geophysics, **78**, no. 3, S137–S155. http://dx.doi.org/10.1190/geo2012-0286.1.

Rosales, D., and J. Rickett, 2001, PS wave polarity reversal in angle-domain common-image gathers: 80th Annual International Meeting, SEG, Expanded Abstracts, http://dx.doi.org/10.1190/1.1816489.

Stewart, R., J. Gaiser, R. Brown, and D. Lawton, 2002, Convertedwave seismic exploration: Methods: Geophysics, **67**, 1348–1363. http://dx.doi.org/10.1190/1.1512781.

Sun, R., G. A. McMechan, H.-H. Hsiao, and J. Chow, 2004, Separating P-and S-waves in prestack 3D elastic seismograms using divergence and curl: Geophysics, **69**, 286–297. http://dx.doi.org/10.1190/1.1649396.

Sun, R., G. A. McMechan, C.-S. Lee, J. Chow, and C.-H. Chen, 2006, Prestack scalar reverse-time depth migration of 3D elastic seismic data: Geophysics, **71**, no. 5, S199–S207. http://dx.doi.org/10.1190/1.2227519.

van der Baan, M., 2006, PP-/PS-wavefield separation by independent component analysis: Geophysical Journal International, **166**, no. 1, 339–348. http://dx.doi.org/10.1111/j.1365-246X.2006.03014.x.

Wang, C., J. Cheng, and B. Arntsen, 2015, Numerical pure wave source implementation and its application to elastic reverse-time migration in anisotropic media: 77th Annual International

Conference and Exhibition, EAGE, Extended Abstracts, http://dx.doi.org/10.3997/2214-4609.201412834.

Wang, C., J. Cheng, and T. Wang, 2014, Local angle domain elastic reverse-time migration in TI media: 76th Annual International Conference and Exhibition, EAGE, Extended Abstracts, http://dx.doi.org/10.3997/2214-4609.20141489.

Yan, J., and P. Sava, 2008, Isotropic angle-domain elastic reverse-time migration: Geophysics, **73**, no. 6, S229–S239. http://dx.doi.org/10.1190/1.2981241.

Zhang, Q., and G. A. McMechan, 2010, 2D and 3D elastic wavefield vector decomposition in the wavenumber domain for VTI media: Geophysics, **75**, no. 3, D13–D26. http://dx.doi.org/10.1190/1.3431045.

Zhang, Q., and G. A. McMechan, 2011, Direct vector-field method to obtain angle-domain common-image gathers from isotropic acoustic and elastic reverse-time migration: Geophysics, **76**, no. 5, WB135–WB149. http://dx.doi.org/10.1190/geo2010-0314.1.